Supporting Information

Strategic Synthesis of Mesoporous Pt-on-Pd Bimetallic Spheres Templated from Polymeric Micelle Assembly

Yunqi Li[a,b], Cuiling Li[a], Bishnu Prasad Bastakoti[a], Jing Tang[a,b], Bo Jiang[a,b], Jeonghun Kim[c], Mohammed Shahabuddin[d], Yoshio Bando[a,b], Jung Ho Kim*[c], and Yusuke Yamauchi*[a,b]

[a] World Premier International (WPI) Research Center for Materials Nanoarchitectonics (MANA), National Institute for Materials Science (NIMS), 1-1 Namiki, Tsukuba, Ibaraki 305-0044 (Japan)

[b] Faculty of Science and Engineering, Waseda University, 3-4-1 Okubo, Shinjuku, Tokyo 169-8555 (Japan)

[c] Institute for Superconducting and Electronic Materials, Australian Institute for Innovative Materials, University of Wollongong, Squires Way, North Wollongong, NSW 2500 (Australia)

[d] Department of Physics and Astronomy, College of Science, PO Box 2455, King Saud University, Riyadh 11451 (Saudi Arabia)

E-mails: jhk@uow.edu.au; yamauchi.yusuke@nims.go.jp

Figure S1

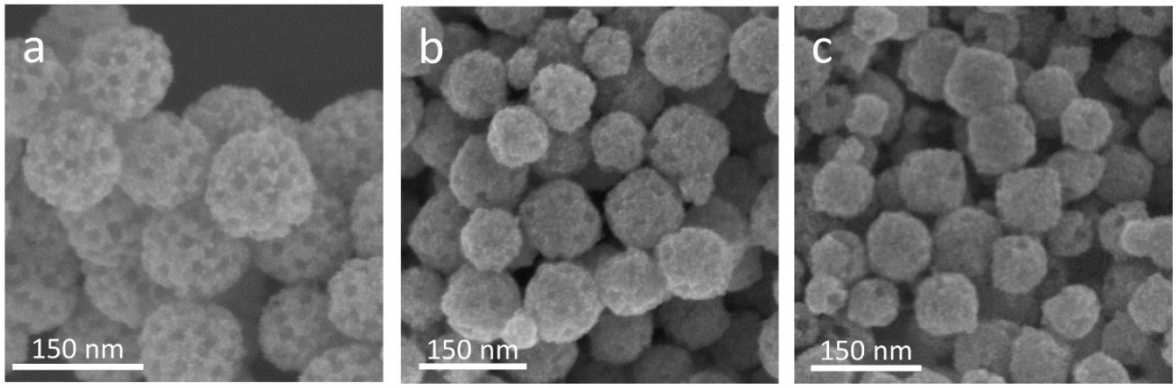

Figure S1. SEM images of mesoporous Pt-on-Pd spheres with different compositions of Pt/Pd = (a) 92/8, (b) 62/38, and (c) 42/58. These three samples were prepared from different precursor solutions of $PtCl_4^{2-}$/$PdCl_4^{2-}$ = (a) 9 : 1, (b) 7 : 3, and (c) 5 : 5, respectively.

Figure S2

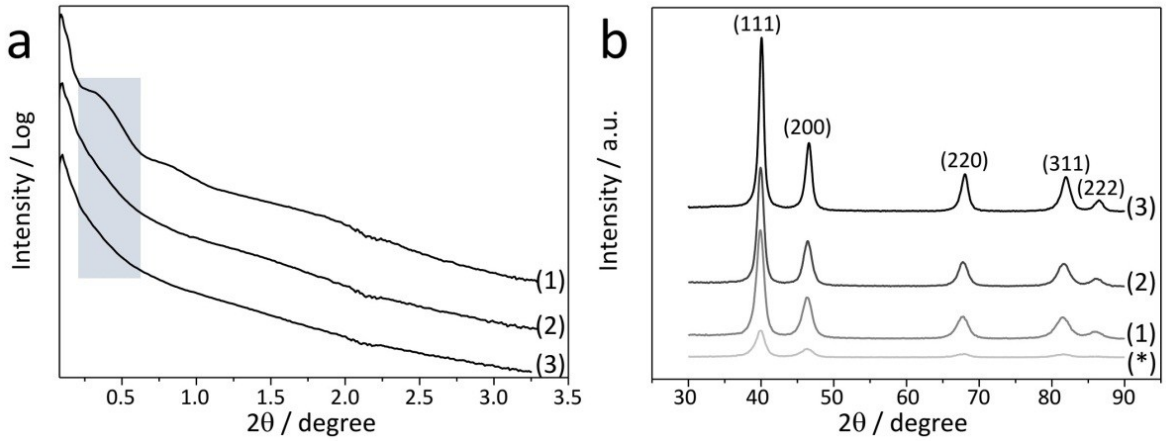

Figure S2. (a) Small-angle XRD patterns and (b) wide-angle XRD patterns of mesoporous Pt-on-Pd spheres with different compositions of Pt/Pd = (1) 92/8, (2) 62/38, and (3) 42/58. For comparison, the wide-angle XRD pattern of mesoporous Pt spheres is also shown as (*).

Table S1. ICP-OES analysis of mesoporous Pt-on-Pd spheres.

Molar ratio of $PtCl_4^{2-}/PdCl_4^{2}$	Compositions of Pt to Pd in mesoporous Pt-on-Pd spheres
10 : 0	100% : 0
9 : 1	92% : 8%
7 : 3	62% : 38%
5 : 5	42% : 58%

Figure S3

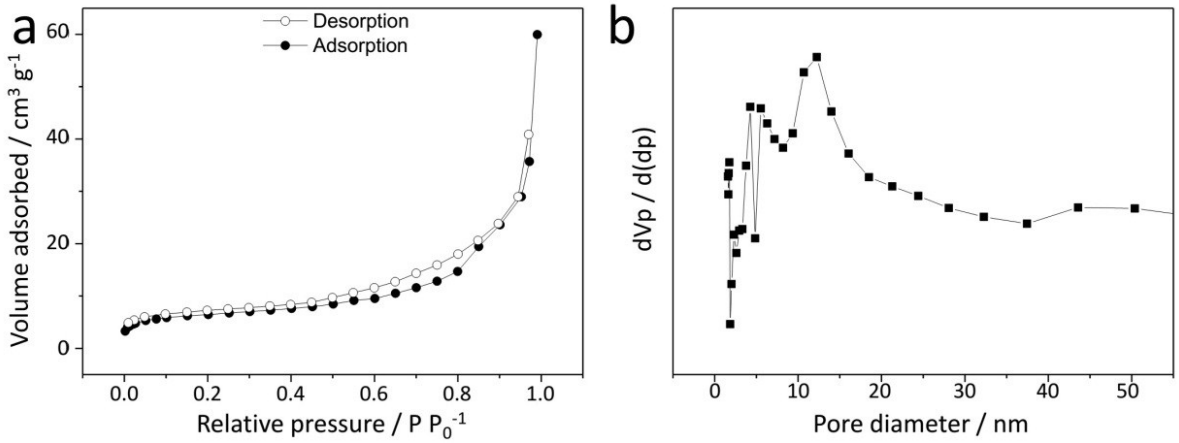

Figure S3. (a) N_2 adsorption-desorption isotherm and (b) BJH pore size distribution curve of mesoporous Pt-on-Pd spheres (Pt/Pd = 92/8) with a dominant pore size of 12 nm.

Figure S4

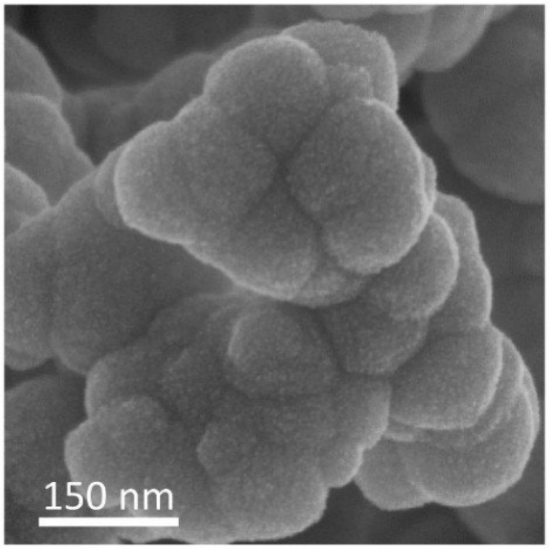

Figure S4. SEM image of corresponding Pt-on-Pd spheres synthesized without using triblock copolymer.

Figure S5

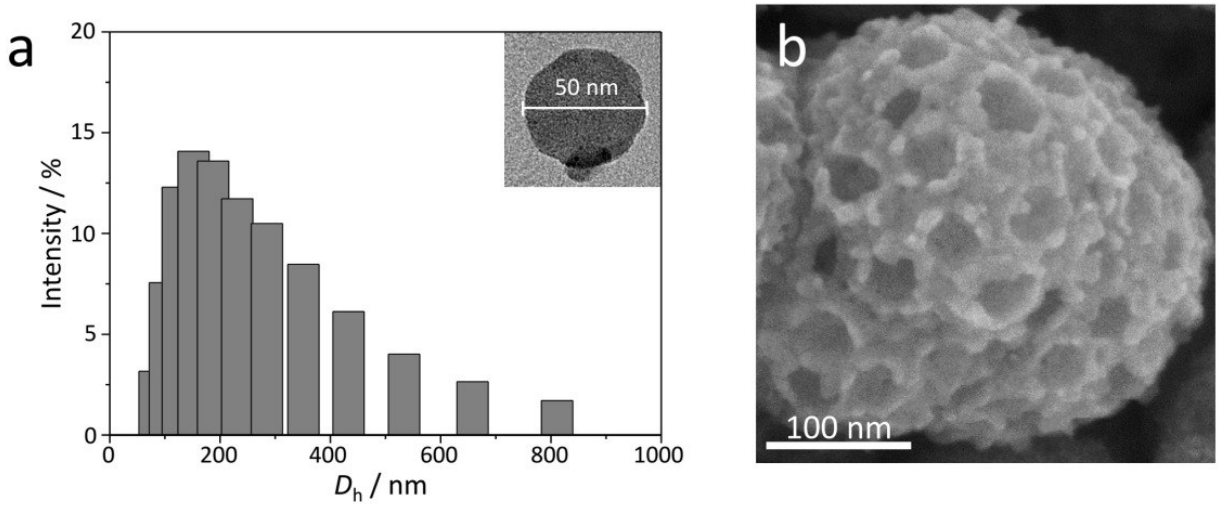

Figure S5. (a) Histogram of size distribution of swollen micelles (inset: TEM image of micelle with a swollen PS core (~ 50 nm), highlighted by 0.1 wt% phosphotungstic acid), and (b) SEM image of huge-sized mesoporous Pt-on-Pd particle obtained from swollen micelles.

Figure S6

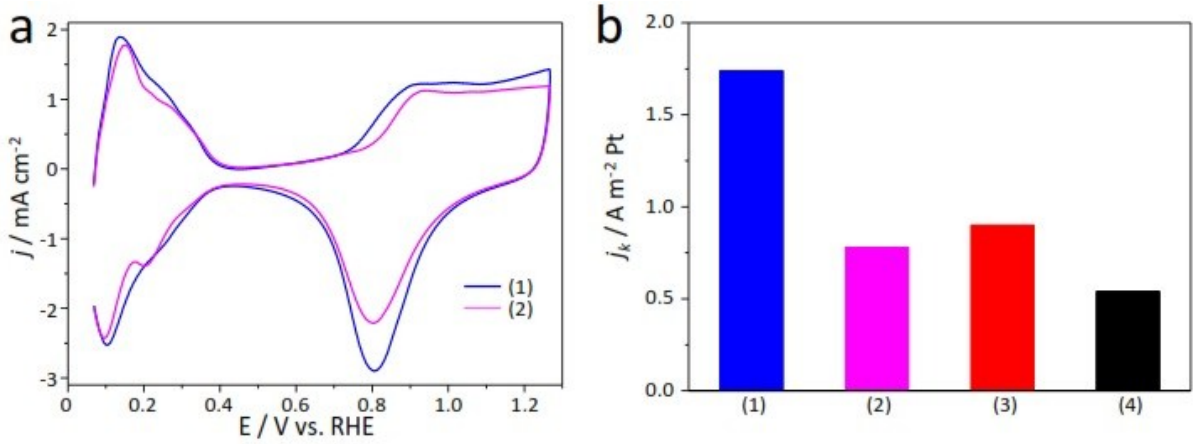

Figure S6. (a) CV curves of (1) mesoporous Pt-on-Pd spheres (Pt/Pd = 92/8), (2) mesoporous Pt, (3) PtC-20% catalyst, and (4) PtB in N_2-saturated 0.1 M $HClO_4$ solution. The ECSAs of mesoporous Pt-on-Pd spheres, and mesoporous Pt spheres are calculated to be 26.1 m^2 g_{Pt}^{-1}, 20.1 m^2 g_{Pt}^{-1}, respectively. (b) Comparison of the specific activities at 0.9 V (*vs.* RHE) normalized by the corresponding ECSAs.

Table S2. Comparison of catalytic activity of mesoporous Pt-on-Pd spheres towards ORR performance with other Pt-Pd based catalysts.

Reference	Material	Onset potential (V vs. RHE)	Half-wave potential (V vs. RHE)	Scan rate (mV s^{-1})	Rotation rate (rpm)
This project	Mesoporous Pt-on-Pd spheres	1.01	0.90	10	1600
J. Mater. Chem. A, 2, 2233-2239, 2014.	Dendritic Pt-on-Pd	1.06	0.87	5	1600
J. Phys. Chem. C, 117, 9826-9834, 2013.	Pt-Pd alloy nanoflowers	0.90	0.84	5	1600
Langmuir, 28, 1579-1587, 2012.	Pt@PdCu/C core-shell structure	0.98	0.89	5	1600
Electrochimica Acta, 152, 417-424, 2015.	Nanoporous PtPd alloy	1.0	0.90	10	1600
Nano Lett., 14, 3570-3576, 2014.	Pt layers on Pd nanocubes	0.85	0.93	-	1600
J. Am. Chem. Soc., 137, 15036-15042.	Pd@Pd decahedra on carbon	0.98	0.92	10	1600

Figure S7

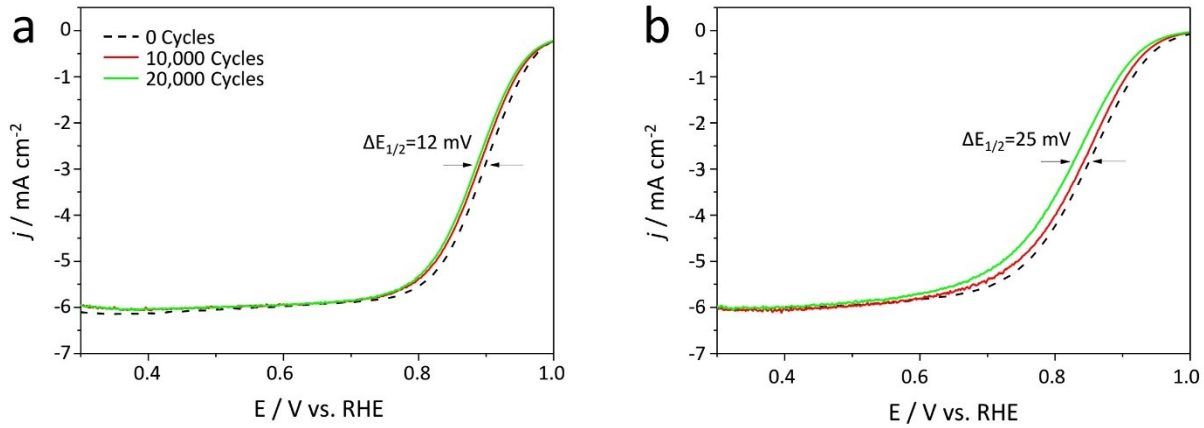

Figure S7. ORR polarization curves obtained in O_2-saturated 0.1 M $HClO_4$ solution at 1,600 rpm after 0, 10000, and 20000 cycles between 0.068 V and 1.268 V (*vs*. RHE) for (a) mesoporous Pt-on-Pd spheres (Pt/Pd = 92/8) and (b) PtC-20% catalyst.

Figure S8

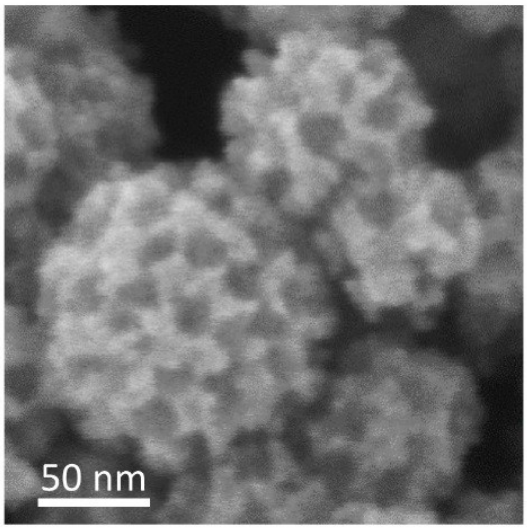

Figure S8. SEM image of mesoporous Pt-on-Pd spheres (Pt/Pd = 92/8) after 20000 potential cycles between 0.068 V and 1.268 V (*vs*. RHE) in O_2-saturated 0.1 M $HClO_4$ solution.